Reference: *Biol. Bull.* **182**: 424–434. (June, 1992)

Causes and Consequences of Fluctuating Coelomic Pressure in Sea Urchins

OLAF ELLERS[1] AND MALCOLM TELFORD[2]

[1]*Department of Zoology, University of California, Davis, California 95616 and*
[2]*Department of Zoology, University of Toronto, Toronto, Ontario M5S 1A1, Canada*

Abstract. We measured coelomic pressure in sea urchins to determine whether it was high enough to support a pneu hypothesis of growth. In *Strongylocentrotus purpuratus* the pressure was found to fluctuate rhythmically about a mean of −8 Pa, and was negative for 70% of the time. This is at variance with the theoretically required positive pressures of the pneu hypothesis. Furthermore, there were no sustained significant differences between the pressure patterns of fed and starved urchins, presumed to be growing and not growing, respectively. The rhythmical fluctuations in pressure were caused by movements of the lantern which changed the curvature and tension of the peristomial membrane. We developed a mathematical and morphological model relating lantern movements, membrane tension, and pressure, that correctly predicts the magnitude of the fluctuations. Pressures predicted by the model depend also on coelomic volume changes. In *Lytechinus variegatus* simultaneous retraction of the podia, which causes expansion of the ampullae, resulted in an 8.8 Pa increase in coelomic pressure, relative to the pressure during simultaneous podial protraction.

Introduction

For some seventy-five years, the growth and shape of sea urchins have, with few exceptions, been attributed to a similarity with internally pressurized tensile structures. D'Arcy Thompson (1917) remarked on the similarity of shape between sea urchins and water droplets on a glass plate. A water-filled balloon resting on a table (Fig. 1) provides an analogous form. This basic idea has been invoked repeatedly to explain both growth and form. Moss and Meehan (1968) suggested that growth of the gut and gonads increased coelomic pressure and this caused growth in the test. Likening echinoids to inflated structures (pneus), Seilacher (1979) argued that variations in shape among regular and irregular echinoids could be explained by forces from the tube feet and by the occurrence of internal "tethers" of calcite or collagen. Dafni and Erez (1982), Dafni (1983, 1985, 1986), and Baron (1988), all assumed the existence of positive internal pressure in sea urchins, and explained morphogenesis in terms of the resulting stress patterns and the action of forces from other sources such as podia, internal muscles, and mesenteries.

Although internal fluid pressure is usually not relevant in the functional analysis of solid structures, there are engineering designs in which it does play an important role. While designing underwater storage vessels that require a minimum of wall materials, Royles *et al.* (1980) were impressed by the similarity of their theoretically derived shapes and some sea urchins (most notably *Echinus esculentus*). The design of such "constant strength" or "buckle-free" structures involves balancing pressure differences (positive or negative) across the vessel wall with forces in the wall. It is tempting to interpret the convergence on an echinoid form as indicative of an underlying similarity in the balance of forces. Royles *et al.* (1980) actually coined the expression of "Echinodome" for these structures.

The obvious and crucial question—what is the magnitude of the internal pressure in echinoids—has not been answered. Dafni (1985, 1986) attempted to manipulate forces acting on the growing test and isolated plates, but provided no measurements of pressure. Reporting the only pressure measurements, Baron (1991) recorded fluctuating coelomic pressures in an echinoid. With the aid of a finite element method he developed a complicated tensile growth model which, although elegantly refined, is still fundamentally a pneu hypothesis. According to his model,

Received 21 October 1991; accepted 27 March 1992.

Figure 1. (a) A balloon filled with water in water; (b) a balloon filled with water in air; and (c) an urchin test. Note the similarity of shape between the (b) and (c). The difference in shape between (a) and (b) illustrates the importance of self-weight forces. There are no self-weight forces on a water-filled balloon in water since the water inside and outside are equally dense. In urchins, the internal volume also has no effective weight; thus the downward forces result only from the underwater weight of the calcite or the pull of tube feet. The weight forces are balanced by internal pressure resulting from tension in the membrane. None of these structures are pneus because they are not air-filled, but (a) and (b) certainly, and (c) possibly, form their shape as a result of forces analogous to those in a pneu, including internal pressurization.

growth can occur only during periods of positive internal pressure.

In this paper we describe a technique for measuring coelomic pressure in sea urchins and report the results of two series of experiments. The first series was undertaken to determine whether there was sufficient positive pressure to support the pneu hypothesis of growth. For this, we compared pressures in sea urchins (*Strongylocentrotus purpuratus*) fed *ad libitum* and presumed to be actively growing, with pressures in starved animals, presumably not growing (Ebert, 1968). After measuring the fluctuating pressures, we investigated the possible morphological and physical causes of the pressure patterns. This led to development of a model relating pressure changes to alterations in curvature in the peristomial membrane during protraction and retraction of the lantern. In the second series of experiments we examined the effect of volume changes, resulting from the alternate extension and retraction of podia, on coelomic pressure in *Lytechinus variegatus*. We consider the interaction of volume changes and behavior of the peristomial membrane in explaining the observed pattern of coelomic pressures in sea urchins.

Materials and Methods

Experimental animals

Specimens of *Strongylocentrotus purpuratus* collected subtidally at Bodega Bay, California, and maintained in running seawater, were divided into two lots. The first was fed *ad libitum* with kelp (*Macrocystis* sp.) and the second was starved. There were no significant differences in the size of urchins in the fed (33.0–81.4 mm, n = 27) and unfed (41.9–82.6 mm, n = 25) groups. Size was estimated by a volume approximation which was (height $\times$ diameter)^2. Pressure measurements were performed during a three-week period, starting two months after the beginning of these feeding regimes. *Lytechinus variegatus* (53.9–68.1 mm diameter) was collected at Long Key, Florida, and maintained on natural substrate with dead leaves of *Thalassia testudinum*, for 12 to 72 h before experimental use.

Pressure measurement

Internal pressure was measured by mounting the urchins on a vertical, 14 gage, hypodermic needle passing through the peristomial membrane. The needle was connected to one side of a P305D differential, moving membrane, pressure transducer (Validyne Corporation, Northridge, California) fitted with a nickel plated 3–20 membrane to read pressures up to $\pm$550 Pa. The other side of the transducer was open to the seawater surrounding the experimental animal.

Calibration of pressure transducer

The system was calibrated before each series of measurements. Calibrations and all experiments were performed in a two-chambered Plexiglas aquarium. At the start, seawater levels in the two chambers were equilibrated via a connecting valve. After closure of the valve, the water

level in one chamber (positive side of transducer) was raised by increments of 1.1 mm by the gradual immersion of a Plexiglas box propelled by a threaded drive mechanism. At each step the voltage output at 1-s intervals was averaged over a 30-s period by a Dynamic Signal Analyzer (Hewlett-Packard #3561A). Initial calibrations were continued to a total pressure head of about 22 mm of seawater (220 Pa). Later calibrations extended only to 11 mm of seawater, which adequately covered the range of pressures commonly encountered. Calibration readings were taken as pressure increased and as it decreased back to zero. Linear regression of transducer output (mv) and pressure, fitted by least squares, was used to convert experimental readings to pressure. For field experiments in Florida, the system was simplified. The Plexiglas box and threaded drive assembly was replaced by a pipetting technique in which 15-ml aliquots of seawater were added sequentially and then removed from the reference chamber.

Estimate of errors in pressure measurements

Due to uncertainty in the measurement of the pressure head against which the transducer was calibrated, the range of bias in the slope of the calibration curve was less than 0.1%. The precision range of the slope was ±10% because of day-to-day variation. Additionally, in the worst case, the 8-bit digitizer recorded only to the nearest 1.7 Pa, and there was drift in the zero; a combined imprecision range of ±3 Pa resulted. The accuracy can be expressed as ±(10.1% + 3) Pa.

We were concerned that urchins might leak, thus artificially relieving high positive or negative pressures. We ruled out this possibility by injecting the urchins with food coloring and by coloring the liquid in the transducer. We observed no color leakage, except at very much higher pressures than those reported in this experiment.

Internal pressure could also be artificially relieved by flow through the needle into the tiny space vacated as the metal membrane of the transducer shifted while making the measurement. This possibility was minimized by use of a "low volume" pressure transducer. To test this potential error, we set up an experiment in which we could simulate the pressure measurement and watch what happened to the pressure and volume. The urchin was replaced by a rubber tube filled with dyed seawater, closed at one end, and attached to a 5 mm diameter graduated pipet that was open to the atmosphere at the other end. With fluid in the pipet levelled to measure 40 Pa, we inserted the needle through the rubber hose. There was no detectable motion of the water level in the pipet, indicating that volume changes due to the transducer motion were less than 3 μl; in a 60 mm diameter urchin, this volume change could be accommodated by a 10 μm upward or downward motion of the lantern involving a strain of 5×10^{-6} in the peristomial membrane, an amount that has a negligible effect on pressure in the coelom.

Experimental procedure

Each urchin, when mounted on the needle, rested on a small platform. The podia reached the platform but could not reach the sides or the floor of the aquarium. During the course of an experiment the transducer output was sampled at 5.12 Hz and digitized. The trace was displayed by the signal analyzer simultaneously with a frequency spectrum. The data were transferred in 200-s sections to an Apple Mac II equipped with a "LabVIEW" GPIB interface card (National Instruments, Austin, Texas). For each urchin, data were recorded for 10 min. The zero point of the transducer was checked after each measurement was completed, and the needle was detached and syringed to remove any coagulated coelomic fluid. Diameter and height of each specimen was measured by calipers. The water in the experimental chamber was replaced after each group of five specimens to minimize changes in water temperature.

The procedure for *L. variegatus* was similar except that a 10 min section of data was transferred directly into the computer, and the light level was manipulated to induce podial movements. For each of ten urchins, room lights and fiber-optic microscope lights directed at the urchin were alternately switched on and off every 2 min. When the lights were on, the podia retracted; when the lights were off, they extended.

Data analysis

For *S. purpuratus* specimens, each 200 s trace was scanned and the following information was compiled: (i) seconds below zero pressure; (ii) the mean pressure; (iii) the standard deviation of pressure; (iv) the maximum pressure; (v) the minimum pressure; (vi) the mean of positive pressures; (vii) the standard deviation of positive pressures; (viii) the mean of negative pressures; (ix) the standard deviation of negative pressures. Two-way analyses of variance by trace and by feeding regime were performed on these data. Additional *t*-tests were performed to compare fed and starved animals by successive traces. A Fourier transform of the third 200-s trace for each specimen gave the amplitude and periodicity of rhythmic pressure fluctuations. Using the first 200-s trace (during which the needle was inserted), a discriminant functions analysis was performed to see whether fed and unfed individuals could be identified from their initial pressure patterns. We performed a stepwise regression to determine which variables to include in the discriminant functions analysis. The discriminant model is

$$Y = b + a_1x_1 + a_2x_2 + a_3x_3 \cdots a_9x_9, \qquad (1)$$

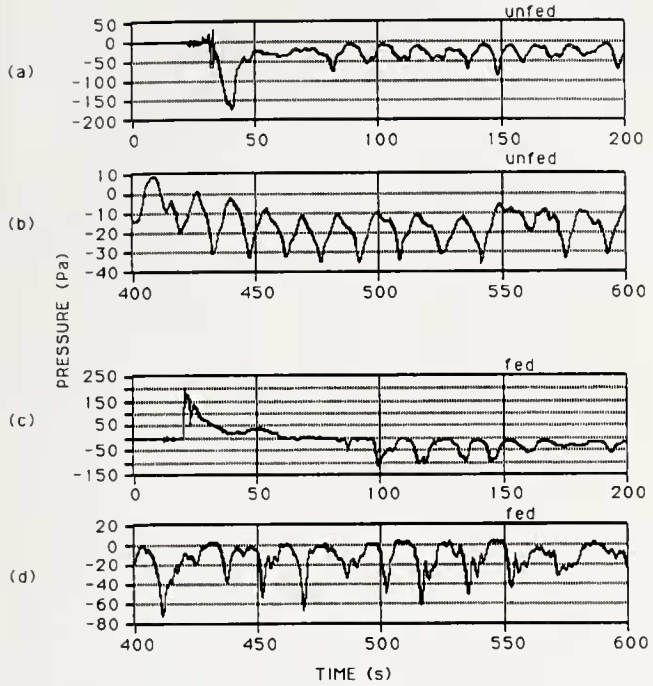

Figure 2. (a) Pressure-time trace for an unfed urchin during the first 200 s of the experiment. The large negative pressure pulse, characteristic of unfed urchins, occurred just after the needle was inserted through the peristomial membrane. (b) Pressure-time trace for an unfed urchin 400–600 s after the start of the experiment. This trace shows the characteristic, rhythmic fluctuations of pressure associated with movements of the lantern. (c) Pressure-time trace for a fed urchin during the first 200 s of the experiment, showing the characteristic, positive pressure pulse as the needle was inserted through the peristomial membrane. (d) Pressure-time trace for a fed urchin 400–600 s after the start of the experiment, showing rhythmical changes with lantern movements. Differences in the traces for starved and fed urchins (a and c) were statistically significant; during the third 200-s traces (b and d) the differences were not significant.

where y is equal to -1 if an urchin is fed, and is equal to $+1$ if an urchin is unfed. The nine variables descriptive of the pressure traces are x_1 to x_9. The fitted slopes are a_1 to a_9 and b is the intercept.

For *L. variegatus* the average level of pressure was measured for each 2-min segment except the first, which was assumed to be a settling-down period. A paired *t*-test was done on the average pressures to compare the lights-off periods with the immediately ensuing lights-on periods.

Results

Description of the pressure traces

Pressure traces for *S. purpuratus* characteristically fluctuated at a frequency of 0.055 Hz with a S.D. of 0.021 Hz (n = 167 traces). This corresponds to an average period of 18 s, and the range of periods corresponding to the above S.D. is 13–29 s.

When the needle was inserted through the peristomial membrane, there was usually a negative or positive pressure peak (Fig. 2) that often went off-scale on the recording equipment, and that differed significantly from the fluctuations in the second and third traces as shown by the maxima and minima in Table I. Over several minutes the pressure tended toward, and eventually stabilized at, an average mean pressure of -8.2 Pa with a S.D. of 11 Pa (n = 52 urchins). According to our error estimate, zero lies in the range $\pm (8.2 \times 10\% + 3)$ Pa: a *t*-test shows that the worst-case zero of -3.8 Pa is significantly different from -8.2 Pa with a S.E. of 1.4 Pa ($P < 0.01$). The average S.D. of the pressure was 10 Pa with S.D. of 6.4 Pa (n = 52). The pressure was below zero 70% of the time.

Urchins fed *ad libitum*, and those receiving food only via occasional cannibalism, had very different initial pressure responses (Fig. 2). Well-fed urchins had pressures that tended to increase initially. Unfed urchins had pressures that tended to decrease initially. All of the variables except S.D. differed significantly in the first 200-s trace (Table I). Step-wise regression of variables for the first trace indicated that the mean of the positive pressures and the minimum pressure ($r^2 = 0.41$, slope significantly non-zero, $P < 0.001$) correctly predicted whether the animals were fed or unfed 83% of the time.

There were no significant correlations between urchin volume and any of the nine descriptive variables in any traces for fed urchins, nor in the first 200-s trace for unfed urchins. However, in subsequent traces from unfed urchins, five of the variables (mean, S.D., minimum, mean negative, and S.D. of negative pressures) were correlated with test size (Table II).

Podial movements and pressure

When the lights were turned off, *L. variegatus* protracted its podia and the coleomic pressure decreased. When the lights were turned on, podia retracted and the coelomic pressure increased (Fig. 3). Coelomic pressure

Table I

Results of t*-tests showing statistically significant differences between fed and starved* Strongylocentrotus purpuratus *for the nine variables descriptive of coelomic pressure during the three successive 200 s traces*

Variable	Trace 1	Trace 2	Trace 3
Seconds below zero	**	n.s.	n.s.
Mean pressure	***	n.s.	n.s.
S.D. pressure	n.s.	n.s.	n.s.
Maximum pressure	**	n.s.	n.s.
Minimum pressure	***	n.s.	n.s.
Mean +ve pressure	***	n.s.	n.s.
S.D. +ve pressure	***	n.s.	n.s.
Mean −ve pressure	**	n.s.	n.s.
S.D. −ve pressure	**	n.s.	n.s.

(n.s. not significant; $^{**}P \leq 0.01$; $^{***}P \leq 0.001$).

Table II

Correlation coefficients between body size and statistical variables descriptive of pressure traces from unfed Strongylocentrotus purpuratus

Variable	Trace 1	Trace 2		Trace 3	
Seconds below zero	n.s.	—	n.s.	—	n.s.
Mean pressure	n.s.	−0.4	*	−0.5	*
S.D. pressure	n.s.	0.4	*	0.4	*
Maximum pressure	n.s.	—	n.s.	—	n.s.
Minimum pressure	n.s.	−0.4	*	−0.5	**
Mean +ve pressure	n.s.	—	n.s.	—	n.s.
S.D. +ve pressure	n.s.	—	n.s.	—	n.s.
Mean −ve pressure	n.s.	−0.5	*	−0.6	**
S.D. −ve pressure	n.s.	0.4	*	0.4	*

(n.s. not significant; $*P \leq 0.05$; $**P \leq 0.01$). Note: There were no correlations between any of these variables and body size in fed urchins.

during the lights-on period was 8.8 Pa higher than the mean pressure during the immediately subsequent lights-off period ($P < 0.0001$; n = 20; 10 urchins, 2 paired samples each).

Discussion

The fluctuating coelomic pressures observed in this study were predominantly negative. In the wide range of animals surveyed by Trueman (1975), most reported pressures are positive, the highest being 10^4 Pa in the lugworm, *Arenicola marina*. In soft-walled pressure vessels, the internal pressure can only be zero or positive relative to the outside. At zero relative pressure, the body wall is limp and any process tending to a negative internal pressure will cause the membrane to collapse and fold, thus reducing the pressure to zero (Clark and Cowey, 1958). Negative pressures are possible in systems in which the walls have flexural stiffness, as is the case with some skeletal and muscular tissues. Trueman (1975) reported pressures of −500 Pa from underneath the foot of *Patella* sp. during the passage of pedal waves. Negative pressures have also been generated inside the gastropod foot (Voltzow, 1986) and by the suckers of an octopus (Kier and Smith, 1990; Smith, 1991). Many soft-bodied animals have some hard, stiff parts, while many primarily hard-bodied organisms have some soft, flexible membranes. Sea urchins, having a hard test and large peristomial membrane, are examples of the latter.

There are several processes that could influence coelomic pressures in sea urchins, but some of them do not produce pressures of the observed magnitude. However, we found two processes of great importance: the exertion of force on the coelomic fluid (for instance, by the peristomial membrane) and the movement of water into the coelomic space (as in the simultaneous retraction of the podia). Before considering these two in more detail, we show why a number of the other possibilities are not significant.

Causes of pressure in urchins

Pressure is a force magnitude per area. In non-accelerating fluids, at each point in the fluid there is a balance of forces in all directions. Gravitational pressure, p_g, at a given depth is

$$p_g = \rho g d, \tag{2}$$

where ρ is the density of seawater, g the acceleration due to gravity, and d the depth (atmospheric pressure is not included). We measured the difference between pressures inside and outside the urchin. Because the two locations were at the same depth, hydrostatic, gravitational pressures are irrelevant, and the remaining discussion refers only to relative transmural pressures.

Sound or sudden impacts from waves could also cause internal pressure. The rhythmic, 20-s pressure patterns we observed cannot be sound because there was no such rhythm when the needle was removed from the urchin. Nevertheless, in the ocean, sudden coelomic pressures from impact forces such as waves and sound are possible and might have implications for behavior, mechanical functioning, or even pressure-regulated growth of urchins. These phenomena have not been investigated.

Hydrodynamic forces are unlikely to be of importance in explaining pressures inside urchins, because rates of flow are very slow. Hanson and Gust (1986) measured rhythmic flows inside urchin coeloms that have the same periodicity (20 s) as the pressure pulses we measured. Thus, fluid dynamic pressures cannot be immediately ruled out in explaining the observed pressure patterns. Expected pressures from flow are less than or equal to the dynamic pressure, p_d, which is

$$p_d = \frac{\rho}{2} u^2, \tag{3}$$

where ρ is the density of seawater, and u is the velocity of flow (Vogel, 1981). In our experimental observations,

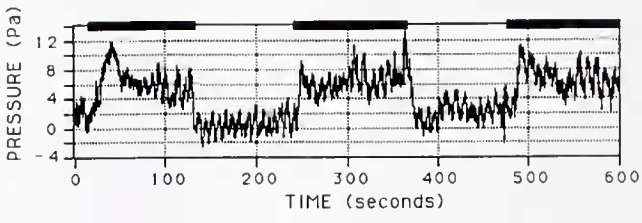

Figure 3. The pressure pattern in *Lytechinus variegatus* when lights are alternately turned on and off at 2-min intervals (black bar indicates lights on). The podia protracted when the light was off and retracted when the light was turned on.

the standard deviation of pressure was 10 Pa. This would correspond to a minimum flow of 100 mm s^{-1}. Because Hanson and Gust (1986) observed a maximum flow of 1.5 mm s^{-1}, we conclude that the pressures we observed were not due to flow.

Tension in a curved, stretched membrane can be another cause of pressure differentials. According to Laplace's law (see Popov, 1976; Wainwright *et al.*, 1976; Vogel, 1988; or Ellers and Telford, 1991), the pressure drop across such a membrane or a flexible body wall depends on its tension and radius of curvature. The pressure inside the membrane will be positive with respect to external pressure when the membrane is inwardly concave. In a cylinder the pressure difference, Δp, across the membrane is

$$\Delta p = \frac{T}{r}, \tag{4}$$

where r is the radius of curvature and T the tension in the membrane. The tension, T, is the stress times the thickness of the material. More generally, in a three-dimensional shape such as a sphere or ellipsoid, two radii of curvature are involved, so that at every point on the surface

$$\Delta p = \frac{T_1}{r_1} + \frac{T_2}{r_2}, \tag{5}$$

where T_1 is the tangential tension in one direction with radius of curvature r_1, and T_2 is the tangential tension in an orthogonal direction, with radius of curvature r_2 (modified from Timoshenko and Woinowsky-Krieger, 1959, p. 435). Both negative and positive differences can occur across a membrane, depending on whether its radii of curvature are positive or negative.

If the several coelomic compartments in echinoids (somatocoels, hydrocoel, axocoel, and peripharyngeal coelom) (Hyman, 1955; Smith, 1984) are bounded by stretched membranes, there is potential for a diversity of pressure relationships between them. We found no reason to suspect that there are more than two functionally pressurized spaces, the water-vascular system and the coelom proper. Injection of red dye confirmed a separate peripharyngeal space, but the membrane is flaccid and flimsy and could not support separate pressurization. The only stretched membranes are found in the peristome, periproct, and water vascular system.

Pressure and peristomial membrane

The peristomial membrane is a circular sheet composed of cross-fiber collagen arrays and circular and radial muscles (Hyman, 1955). In some species, it contains calcite plates or spicules (Smith, 1984; Candia Carnevali *et al.*, 1990). It is joined to the test at the distal edge, and to the lantern centrally. Thus the shape of the membrane is like a washer: flat, with a hole in the middle. No one has studied the deformation of this membrane as the lantern protracts and retracts, but from our pressure measurements and the general rules about membranes given above, we can make predictions about its curvature.

Curvature of the membrane depends on the relative pressure difference across it. As the lantern protracts, the pressure inside becomes negative relative to ambient. From Laplace's law, we know that a negative internal pressure implies that the membrane is convex on the coelomic side. Conversely, a positive internal pressure would imply that the membrane is concave on the coelomic side. The same is true for the periproctal membrane. In species in which the periproct is flexible, its shape might indicate a positive or negative internal pressure. These predictions hold only if the membranes have low flexural stiffness. Often flexural stiffness may be conferred by catch-collagen or ossicles. If the membranes are flexurally very stiff, then they may produce negative or positive pressures regardless of their curvature, just as the test does not reverse its curvature as internal pressure changes from positive to negative. It should be a goal of future studies to determine the flexural stiffness of such membranes.

Regardless of the membrane curvature and flexural stiffness, protractor and retractor muscles controlling the motion of the lantern exert forces that cause tension in the peristomial membrane and thus a pressure drop across it. We observed the lantern moving in and out during our pressure measurements, and the 20-s pressure rhythm appeared to match its protraction and retraction. Jensen (1985) suggests that the role of such lantern movements is to stir the coelomic fluid, thus facilitating distribution of nutrients and respiratory gases.

Pressure and podial movements

When many podia simultaneously retract, water previously in the podia will be stored in the ampullae, thus effectively moving water into the coelomic space. If the peristomial membrane and periproct do not move compensatorily outward, and if there is negligible flow via the madreporite, the pressure in the coelom must rapidly increase. In fact, because of the incompressibility of water, if there is no volume regulation the urchin must either spring a leak or the pressure would become so great that the podia could not retract. Fechter (1965) recognized this problem. He calculated that the volume made available when the peristomial membrane moves outward is sufficient to compensate for the volume of water moved into the coelomic space when all podia simultaneously contract. Further, he showed that the size of the peristomial membrane was more closely correlated with the number of podia than with test size. Finally, he demon-

strated only very small flows via the madreporite during simultaneous podial retraction. We observed that simultaneous podial retraction caused an 8.8 Pa pressure increase in the coelom. Fechter (1965), working with *Echinus esculentus*, reported an increase of 200 Pa.

Although the madreporite is not involved in volume-related pressure regulation, Fechter (1965) concluded that it was involved in non-volume-related changes due to gravitational, hydrostatic pressure. We believe that Fechter's conclusion must be wrong, but first we will present his experimental evidence. Fechter glued the madreporite shut and performed two manipulations. (1) He increased the hydrostatic, gravitational pressure by increasing the depth at which the urchin was kept. When the external pressure increased the podia collapsed. (2) He pulled the lantern outward, decreasing the pressure in the coelom, and again the tube feet collapsed.

In the second case, the madreporite could not relieve the induced pressure change because, according to Fechter's own results, it allows insufficient flow. We argue, instead, that pulling the peristomial membrane outwards causes a volume flow from the podia into the ampullae. In the first case, when hydrostatic pressure increases, it does so with negligible volume change. Therefore, although the increase in hydrostatic pressure may be sufficient to cause the podia to collapse, it would do so only if the pressure was being relieved by a flow from the podia into the ampullae. But because this pressure change is gravitational, it is not associated with a volume change, and therefore even the tiniest flow from the podia into the ampullae will immediately relieve the pressure difference.

The only way we can explain Fechter's results is if there was an air bubble in the coelom that would have diminished in size with increasing gravitational pressure, therefore causing flow from the podia into the ampullae. Such air bubbles sometimes form in urchins that have been in air for some time. Fechter dried the madreporite with a stream of hot air, before gluing it shut. Perhaps this procedure explains his results. We suggest that, contrary to Fechter's conclusion, his experiments do not show that the madreporite functions to accommodate hydrostatic gravitational pressures. Furthermore, such a function is unnecessary because volume changes caused by hydrostatic pressure would be accommodated by miniscule flows and deformation of tissues.

Although accommodation of hydrostatic, gravitational pressure is unnecessary, there are other types of pressure that might require the coelomic pressure to be maintained independent of the water-vascular system, and perhaps the madreporite has such a role. For instance, the pressure fluctuations we observed (±10 Pa) could have caused the podia to malfunction because these pressures would be exerted on the ampullae inside the coelom. But such fluctuations can only cause podia to extend or retract if they cause the ampullae to expand or contract, which would happen only if volume changes were associated with the pressure fluctuations. Additionally, the deformation of a membrane depends on its stiffness and on radius of curvature [as in equations (4) and (5), above]. The radius of curvature of the ampullae is much smaller than that of the peristomial membrane, and therefore we expect much smaller deformations in the ampullae. That the ampullae have a smaller radius of curvature than the peristomial membrane may be a design requirement of echinoderm water-vascular systems.

The digestive tract is another potential source of pressure change. When full, the stomach will take up more room in the coelom, and the peristomial membrane must move outwards to relieve the volume increase. Similarly, flows into and out of the mouth, or in the siphon, may cause volume fluctuations that could cause pressure changes if the peristomial membrane does not move compensatorily. Further, without compensation by the peristomial membrane, defecation may lower coelomic pressure because it tends to reduce the volume of gut contents.

Finally, several authors have described ruffled sacs hanging externally from the peristomial membrane (Hyman, 1955; Smith, 1984), the supposed function of which is either as gills or pressure regulators for the peripharyngeal coelom. However, no experimental data about their function have been presented. We saw no evidence that these sacs expanded or contracted while the coelomic pressure fluctuated. Furthermore, their openings are far too small to allow sufficient flow to regulate coelomic volume.

A model of forces causing a pressure drop across the peristomial membrane

The forces causing protraction of the lantern, and thus tension in the peristomial membrane, come from lantern protractor and retractor muscles and from the submerged weight of the lantern. These forces must be estimated. Andrietti *et al.* (1990) report 3 g (0.03 *N*) for lantern weight minus buoyancy in a specimen of *Paracentrotus lividus*. They also report forces of 40 g (0.4 *N*) exerted by lantern protractors and forces of 10 g (0.1 *N*) exerted by lantern retractor muscles. Because *P. lividus* rarely exceeds 70 mm diameter (Mortensen, 1977), it is similar in size to *S. purpuratus* and *L. variegatus*, and the forces should be comparable.

The assumed geometry of the lantern, test and peristomial membrane are shown in Figure 4a. The forces on the peristomial membrane are: (1) a vertical force, f_v, exerted by the lantern weight and the lantern muscles; (2) forces from the pressure difference across the membrane; and (3) the reactive, tensile force exerted on the membrane

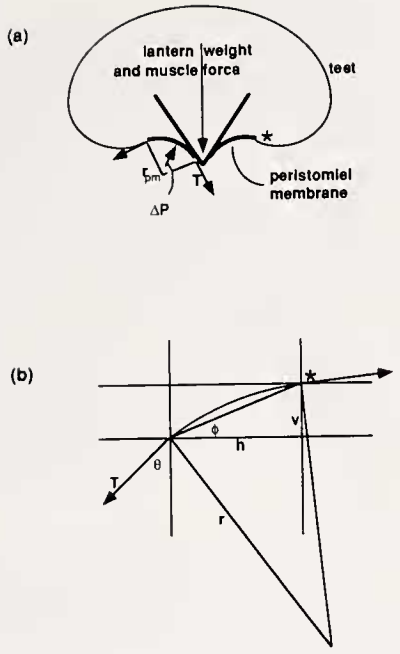

Figure 4. (a) Location of the peristomial membrane in an urchin. The star in both figures marks the point of attachment to the edge of the peristome. (b) Geometric model of the peristomial membrane. The angle θ, and the radius of curvature of the membrane are not independent. Zero vertical displacement occurs when the membrane is horizontal.

by the test. The vertical force, f_v, exerts a force, f_m, in the membrane,

$$f_m = \frac{f_v}{\cos(\theta)}, \tag{6}$$

where θ is the angle between the vertical and a tangent at the central margin of the membrane (at the point of attachment of the peristomial membrane to the teeth) (Fig. 4b). The force, f_m, on the membrane corresponds to a tension, $\mathbb{T}$, (force per length) in the membrane of

$$\mathbb{T} = \frac{f_m}{(2\pi r_t)}, \tag{7}$$

where r_t is the radius of the central margin of the peristomial membrane. From Laplace's equation (4)

$$\Delta p = \frac{\mathbb{T}}{r_{pm}}, \tag{8}$$

where r_{pm} is the radius of curvature of the membrane. In using equation (4) rather than (5) we make two simplifying assumptions: that a second horizontal radius of curvature can be ignored, and that the curve formed by a vertical cross section of the peristomial membrane has a single radius of curvature at every point. In reality this curve may have variable radii of curvature. A more realistic model would add an unjustifiable degree of complexity for the present context. The two-dimensional approach used here should give results of the correct order of magnitude.

The radius of curvature of the peristomial membrane, r_{pm}, for a given protraction of the lantern, v, and a given horizontal, peristomial radius, h, can be derived from the geometry shown in Figure 4b. The radius of curvature is

$$r_{pm} = \frac{h}{2\cos(\arctan(v/h))\cos(\theta + \arctan(v/h))}. \tag{9}$$

Substituting through equations 6, 7 and 8,

$$\Delta p = \frac{f_v \cos(\arctan(v/h))\cos(\theta + \arctan(v/h))}{\pi h r_t \cos(\theta)}, \tag{10}$$

which is shown in Figure 5. This graph shows that many possible combinations of pressure, protraction, and θ are possible when only the force balance on the membrane is considered. Initially, this may seem counterintuitive. Intuition suggests that as the lantern protracts, the internal pressure should get more and more negative relative to outside as the membrane pulls more and more on the constant volume of water inside the urchin. That this pressure pattern is not implied in Figure 5 reflects the fact

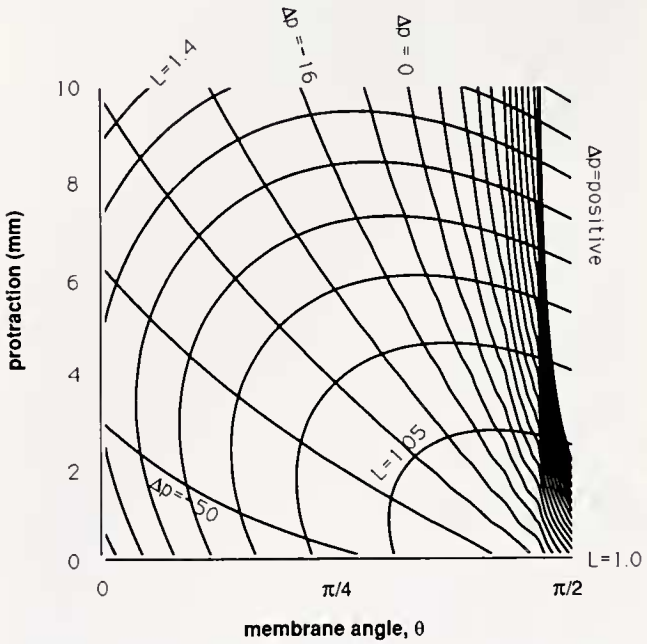

Figure 5. Contour plot of theoretical predictions from the geometric, force balance model of the peristomial membrane (see Fig. 4 and text for details). Elongation of the peristomial membrane and pressure across it are functions of the membrane angle at the central edge, θ, and protraction, v, given a downward force of the teeth and lantern muscles on the membrane, f_v. This graph shows that many combinations of θ and v are possible at a given pressure across the membrane. Which θ, v path the membrane follows as the lantern protracts depends on the volume of the urchin and the properties of the peristomial membrane.

that the force balance makes no assumption about the volume of water inside the urchin, nor about the material properties of the peristomial membrane.

To understand a fluctuating pattern of pressure becoming increasingly negative as the lantern protracts, examine the change in length of the peristomial membrane. The length of the membrane, the distance along its vertical arc from the attachment point at the test to its attachment point at the teeth, is

$$\mathbb{L}_{pm} = r_{pm}(\pi - 2(\theta + \phi)) \qquad (11)$$

(the angle ϕ is shown in Fig. 4b).

By examining the contour plots of pressure drop, and peristomial membrane length (Fig. 5), it is possible to imagine what is happening as the lantern moves. As it protracts, the peristomial membrane elongates, and, assuming constant coelomic volume, the internal pressure must decrease. Initially, assume that the membrane starts at the point, $\theta = \pi$ radians (the membrane is straight and horizontal). As the lantern protracts, the line representing the motion of the lantern must move towards higher v (protraction) and towards lower θ on the graph, to stay in the region of negative pressure and simultaneously to increase the length of the peristomial membrane. Increase in the length of the peristomial membrane helps to compensate for volume changes that would otherwise occur because it can arch upward, effectively compensating for the volume of the lantern pulled downward.

According to Figure 5, the tendency to decrease θ while increasing v, initially causes Δp to become negative quickly because many pressure contour lines must be crossed, but, after even a little protraction, it is possible for the lantern to protract and follow an isobar. This may be an explanation for the plateaus often observed at the peaks of fluctuations in the pressure trace. A path followed by the lantern could be specified by two functions of time, θ(time) and v(time), which we call a "θ, v" path. This path, represented by an imaginary line in Figure 5, will depend on the constraints imposed by the degree of constancy of the coelomic volume and the material properties of the peristomial membrane. We plan to develop this theoretical model further in the future and obtain measurements of the motion of the lantern, the constancy of the coelomic volume, and the material properties of the peristomial membrane.

This crude, initial model serves to explain some aspects of the relationship between pressure and the behavior of the structures that cause it. The pressures are of the correct order of magnitude to have been caused by lantern muscles. The mean negative pressure observed (−8 Pa) is small enough that it could have been caused by the weight of the lantern. If the podia simultaneously retract, or if the stomach is full, thus raising the coelomic volume, this model shows that the lantern can still protract with only a change in the θ, v path. Finally, it is reasonable to calculate the pressure based solely on what the peristomial membrane is doing, because the pressure inside the urchin's coelom is the same everywhere, and thus if any other structure were contributing, it would have to be balanced by tension in the peristomial membrane.

Implications of the observed pressures for the pneu theory

In keeping with the pneu hypothesis, we expected continuously positive internal pressure in sea urchins. Instead we found fluctuating positive and negative pressures, with an overall mean below zero. Clearly, the original version of the pneu hypothesis must be rejected on the basis of these measurements.

Baron (1991) also recognized the problem for the pneu hypothesis when he found fluctuating pressures. He developed a modified version of the hypothesis that preserves the spirit of the original (Thompson, 1917) but incorporates new rules for growth of the skeleton. Baron (1991) proposed that skeletal plates grow at their margins whenever they are in tension, and that growth is directly proportional to tensile stress. Instead of the term "pneu," he called this a "tensile growth model." These growth rules necessitated development of a finite element analysis to determine the expected stresses in the skeleton caused by internal pressure and other forces, such as those from tube feet. From these analyses Baron (1991) was able to generate urchin-like shapes using a computer. Making several alternative assumptions about internal pressure, he examined their effect on the shapes produced by his model. In these simulations, he found that a pressure fluctuating about a mean of 30 Pa, with a S.D. of 30 Pa, generated a shape indistinguishable from that produced with a constant pressure of 30 Pa. Based on this finding, he thereafter simulated urchin shapes using constant pressures.

Baron's (1991) assumptions can be compared with our more extensive pressure measurements. For his standard growth situation he assumed a pressure of 30 Pa, and the other pressure used was 15 Pa. We observed an average pressure of −8 Pa. Under fluctuating pressure regimes he assumed a negative pressure for at most 17% of the time, whereas we observed it for 70% of the time. Baron's (1991) model allowed growth whenever the skeleton was in tension due to internal pressure. This implies that during periods of no growth, the pressure must be lower. But we found that in well-fed, growing (Ebert, 1968) and starved, possibly shrinking, urchins (Levitan, 1988; 1989), the mean pressures were equal after the initial pressure surges in the first 200-s traces (Table I).

The discrepancies between our observations and Bar-

on's (1991) assumptions have two possible implications: that our specimens were abnormal, or that his assumptions do not reflect the pressure patterns in real urchins. In the latter case, it may be that the spirit of the pneu hypothesis is wrong, or that Baron's (1991) version does not incorporate exactly the right assumptions. These possibilities can only be resolved by further experiments and more refined theories.

At present, the most detailed predictions of urchin shape, based on Baron's (1991) tensile growth model, deal only with regular urchins. A challenge to all models is the great diversity of forms that must be generated, including flattened sand dollars (Clypeasteroida), heart urchins (Spatangoida), and the bizarre flask-shaped pourtalesiids (Holectypoida).

Acknowledgments

This work was supported by University of California, Davis, Agricultural Experiment Station Project no. 5134-H and a U. C. Davis, Bodega Marine Laboratory Travel Grant to O. Ellers; and a Natural Sciences and Engineering Research Council of Canada Grant (#A4696) to M. Telford. We thank Bodega Marine Laboratory for use of their facilities. We specially thank K. Brown for her organizational help and H. Fastenau for diving to collect the urchins and subsequently caring for and feeding them. We thank J. Swanson and the staff of Keys Marine Laboratory, Florida, for the use of their facilities and help in collecting urchins. Thanks also to M. Martinez and K. Driver who assisted in some of the experiments and to D. Levitan who critically read the manuscript.

Literature Cited

Andrietti, F., M. D. Candia Carnevali, I. C. Wilkie, G. Lanzavecchia, G. Melone, and F. C. Celentano. 1990. Mechanical analysis of the sea-urchin lantern: the overall system in *Paracentrotus lividus*. *J. Zool. Lond.* **220**: 345–366.

Baron, C. J. 1988. Do mechanical forces explain patterns of growth and form in sea urchins? A finite element analysis. *Proc. Int. Echinoderms Conf., Victoria, Canada* **1987**: 786.

Baron, C. J. 1991. The structural mechanics and morphogenesis of extant regular echinoids having rigid tests. Ph. D. Dissertation, University of California, Berkeley. 269 pp.

Candia Carnevali, M. D., F. Bonasoro, F. Andrietti, and G. Melone. 1990. Functional morphology of the peristomial membrane of regular sea urchins: structural organization and mechanical properties in *Paracentrotus lividus*. Pp. 207–216. in *Echinoderm Research*, De Ridder, Dubois, Lahaye and Jangoux, eds. Balkema, Rotterdam.

Clark, R. B., and J. B. Cowey. 1958. Factors controlling the change of shape of certain nemertean and turbellarian worms. *J. Exp. Biol.* **35**: 731–748.

Dafni, J. 1983. Aboral depressions in the tests of the sea urchin *Tripneustes cf. gratilla* (L.) in the gulf of Eilat, Red Sea. *J Exp. Mar. Biol. Ecol.* **67**: 1–15.

Dafni, J. 1985. Effect of mechanical stress on the calcification pattern in regular echinoid skeletal plates. *Proc. Int. Echinoderms Conf., Galway* **1984**: 233–236.

Dafni, J. 1986. A biomechanical model for the morphogenesis of regular echinoid tests. *Paleobiology* **12**(2): 143–160.

Dafni, J., and J. Erez. 1982. Differential growth in *Tripneustes gratilla* (Echinoidea). *Proc. Int. Echinoderms Conf., Tampa Bay* **1981**: 71–75.

Ebert, T. A., 1968. Growth rates of the sea urchin *Strongylocentrotus purpuratus* related to food availability and spine abrasion. *Ecology* **49**: 1075–1091.

Ellers, O., and M. Telford. 1991. Forces generated by the jaws of clypeasteroids (Echinodermata: Echinoidea). *J. Exp. Biol.* **155**: 585–603.

Fechter, H. 1965. Über die Funktion der Madreporenplatte der Echinoidea. *Z. Verg. Physiol.* **51**: 227–257.

Hanson, J. L., and G. Gust. 1986. Circulation of perivisceral fluid in the sea urchin *Lytechinus variegatus*. *Mar. Biol.* **92**(1): 125–134.

Hyman, L. H. 1955. *The Invertebrates: Echinodermata. The Coelomate Bilateria*, Volume IV, McGraw-Hill, New York. 763 pp.

Jensen, M. 1985. Functional morphology of test, lantern, and tube feet ampullae system in the flexible and rigid sea urchins (Echinoidea). *Proc. Int. Echinoderms Conf., Galway* **1984**: 281–288.

Kier, W. M., and A. M. Smith. 1990. The morphology and mechanics of octopus suckers. *Biol. Bull.* **178**: 126–136.

Levitan, D. R. 1988. Density-dependent size regulation and negative growth in the sea urchin *Diadema antillarum* Philippi. *Oecologia* **76**: 627–629.

Levitan, D. R. 1989. Density-dependent size regulation in *Diadema antillarum*: effects on fecundity and survivorship. *Ecology* **70**(5): 1414–1424.

Mortensen, Th. 1977. *Handbook of the Echinoderms of the British Isles*. Dr. W. Backhuys, Uitgever, Rotterdam. 471 pp.

Moss, M. L., and M. M. Meehan. 1968. Growth of the echinoid test. *Acta Anatom.* **64**: 409–444.

Popov, E. P. 1976. *Mechanics of Materials*, 2nd ed. Prentice-Hall, Englewood Cliffs, NJ. 590 pp.

Royles, R., A. B. Sofoluwe, M. M. Baig, and A. J. Currie. 1980. Behavior of underwater enclosures of optimum design. *Strain* January, 1980, pp. 12–20.

Seilacher, A. 1979. Constructional morphology of sand dollars. *Paleobiology* **5**(3): 191–221.

Smith, A. B. 1984. *Echinoid Palaeobiology*. George Allen and Unwin, London. 190 pp.

Smith, A. M. 1991. Negative pressure generated by octopus suckers: a study of the tensile strength of water in nature. *J. Exp. Biol.* **157**: 257–271.

Thompson, D. W. 1917. *On Growth and Form*. Cambridge University Press, London.

Timoshenko, S., and S. Woinowsky-Krieger. 1959. *Theory of Plates and Shells*, 2nd ed. McGraw-Hill, New York. 580 pp.

Trueman, E. R. 1975. *The Locomotion of Soft-bodied Animals*. Edward Arnold, London. 200 pp.

Vogel, S. 1981. *Life in Moving Fluids*. Willard Grant Press, Boston. 352 pp.

Vogel, S. 1988. *Life's Devices*. Princeton University Press, Princeton, NJ. 367 pp.

Voltzow, J. 1986. Changes in pedal intramuscular pressure corresponding to behavior and locomotion in the marine gastropods *Busycon contrarium* and *Haliotis kamptschatkana*. *Can. J. Zool.* **64**(10): 2288–2293.

Wainwright, S. A., W. D. Biggs, J. D. Currey, and J. M. Gosline. 1976. *Mechanical Design in Organisms*. Princeton University Press, Princeton, NJ. 423 pp.

Appendix 1

List of theoretical variables

Δp, pressure drop across a membrane
T, tension in the membrane
r, radius of curvature
T_1, tangential tension in one direction in the membrane,
r_1, radius of curvature associated with T_1
T_2, tangential stress in the direction perpendicular to T_1
r_2, radius of curvature associated with T_2
p_g, gravitational pressure, (not including atmospheric pressure)
d, water depth
ρ, density of seawater
g, acceleration due to gravity
p_d, dynamic pressure
u, speed of flow
f_v, vertical force exerted on the membrane by the lantern weight and muscles
f_m, is the tangential force in the membrane at the membrane's attachment to the teeth
θ, angle of membrane's attachment to the lantern (see Fig. 5b), same as tangential angle defined by f_m
$\mathbb{T}$, tension in the membrane
r_l, radius of the central margin of the peristomial membrane
r_{pm}, radius of curvature of the peristomial membrane
v, lantern protraction distance
h, horizontal distance from the central margin to the distal margin of the peristomial membrane.
$\mathbb{L}$, arc length of the peristomial membrane
ϕ, see diagram in Figure 5b.
θ, v path—the combination of θ and v used by the membrane as it protracts